ChemPhysChem

Research Article
doi.org/10.1002/cphc.202300100

Chemistry Europe
European Chemical Societies Publishing

www.chemphyschem.org

Redox Properties and in Vivo Magnetic Resonance Imaging of Cyclodextrin-Polynitroxides Contrast Agents

Lorenzo Franco,*[a] Abdirisak Ahmed Isse,[a] Antonio Barbon,[a] Lina Altomare,[b] Viivi Hyppönen,[c] Jessica Rosa,[c] Venla Olsson,[d] Mikko Kettunen,*[c, e] and Lucio Melone*[b, f]

This paper reports the synthesis, characterization and *in vivo* application of water-soluble supramolecular contrast agents (Mw: 5–5.6 kDa) for MRI obtained from β-cyclodextrin functionalized with different kinds of nitroxide radicals, both with piperidine structure (**CD2** and **CD3**) and with pyrrolidine structure (**CD4** and **CD5**). As to the stability of the radicals in presence of ascorbic acid, **CD4** and **CD5** have low second order kinetic constants ($\leq$ 0.05 $M^{-1}s^{-1}$) compared to **CD2** (3.5 $M^{-1}s^{-1}$) and **CD3** (0.73 $M^{-1}s^{-1}$). Relaxivity (r_1) measurements on compounds **CD3**-**CD5** were carried out at different magnetic field strength (0.7, 3, 7 and 9.4 T). At 0.7 T, r_1 values comprised between 1.5 $mM^{-1}s^{-1}$ and 1.9 $mM^{-1}s^{-1}$ were found while a significant reduction was observed at higher fields ($r_1 \approx$ 0.6-0.9 $mM^{-1}s^{-1}$ at 9.4 T). Tests *in vitro* on HEK293 human embryonic kidney cells, L929 mouse fibroblasts and U87 glioblastoma cells indicated that all compounds were non-cytotoxic at concentrations below 1 $\mu mol\,mL^{-1}$. MRI *in vivo* was carried out at 9.4 T on glioma-bearing rats using the compounds **CD3**-**CD5**. The experiments showed a good lowering of T_1 relaxation in tumor with a retention of the contrast for at least 60 mins confirming improved stability also in vivo conditions.

Introduction

Contrast agents (CA) for magnetic resonance imaging (MRI) are widely used in clinical practice to improve diagnostic accuracy.[1,2] Despite the success of gadolinium (III)-chelate-based CAs due to their excellent relaxation properties, some safety concerns have been raised. In particular, side effects have been reported in the case of patients with unpaired kidney function.[1,3–5] Moreover, a long-term retention of Gd-CAs in tissues and organs, brain in particular, has been described.[6,7] In 2017 the European Medicines Agency (EMA) recommended to restrict or to suspend the use of some Gd-CAs based on linear chelates "*in order to prevent any risks that could potentially be associated with gadolinium brain deposition*".[8] During the last years the development of metal-free CAs based on nitroxide radicals (NRs) has therefore become an active and interesting research field. Being biologically relatively safe,[9] NRs might represent an important alternative to the Gd-CAs.[10–13] Moreover, NRs have been proposed in tissue engineering applications as probes for the *in vivo* tracking of hydrogels that act as carriers for the delivery of bioactive factors.[14,15] Finally, taking advantage of the reversible redox properties of NRs, they have been proposed as sensors for monitoring the redox imbalance and the oxidative stress in pathological tissues *in vivo*.[16]

However, NRs are not free of limitations. Their longitudinal relaxivity (r_1) is about 0.2 $mM^{-1}s^{-1}$, a value much lower than the one associated with Gd-CAs ($\approx$3–6 $mM^{-1}s^{-1}$). To overcome this drawback, researchers have designed supramolecular polynitroxides in which a single (macro)molecule bears multiple radical units. This approach allows to enhance the local concentrations of radicals and to decrease their diffusional and rotational motion which leads to an improvement of the relaxation capability.[17–27]

[a] *Prof. L. Franco, Prof. A. A. Isse, Prof. A. Barbon*
Department of Chemical Sciences
University of Padova
Via Marzolo 1, 35131 Padova, Italy
E-mail: lorenzo.franco@unipd.it

[b] *Prof. L. Altomare, Prof. L. Melone*
Department of Chemistry, Materials and Chemical Engineering "G.Natta"
Politecnico di Milano
Via Mancinelli 7, 20131, Milano, Italy
E-mail: lucio.melone@polimi.it

[c] *MSc. V. Hyppönen, Dr. J. Rosa, Prof. M. Kettunen*
Metabolic MR Imaging, A.I. Virtanen Institute for Molecular Sciences
University of Eastern Finland
Neulaniementie 2, 70211, Kuopio, Finland
E-mail: mikko.kettunen@uef.fi

[d] *Dr. V. Olsson*
Molecular Medicine, A.I. Virtanen Institute for Molecular Sciences
University of Eastern Finland
Neulaniementie 2, 70211, Kuopio, Finland

[e] *Prof. M. Kettunen*
Kuopio Biomedical Imaging Unit, A.I. Virtanen Institute for Molecular Sciences
University of Eastern Finland
Neulaniementie 2, 70211, Kuopio, Finland

[f] *Prof. L. Melone*
Centro di Ricerca per l'Energia, l'Ambiente e il Territorio (CREAT)
Università Telematica eCampus
Via Isimbardi 10, 22060, Novedrate, Italy
E-mail: lucio.melone@uniecampus.it

Supporting information for this article is available on the WWW under https://doi.org/10.1002/cphc.202300100

A further aspect that has impeded the translation of NRs into the clinical application is the low stability of some radicals after their *in vivo* administration. For example, the nitroxide most commonly investigated, 2,2,6,6-tetramethylpiperidinyl-1-oxyl (TEMPO), once injected into the body, easily loses its paramagnetic character because it is rapidly reduced to its corresponding hydroxylamine. During the years, several research groups have developed NRs that are less prone to the reduction. It has been found that NRs with a five-membered ring (pyrrolidine structure) are much more stable than those having a six-membered ring (piperidine structure). The stability is further enhanced by the presence of bulky substituents (ethyl or cyclohexyl groups in place of methyl groups).[28–30]

The recent progress on the development of multifunctional nanoprobes for biological imaging from polysaccharides has been described in a very recent and interesting review.[31] Indeed, the combination of polysaccharides and CAs allows to construct macromolecules for imaging applications with improved biocompatibility, biodegradability, and solubility. In 2020 our group reported the synthesis of water-soluble supramolecular polynitroxides obtained from cyclodextrins (CDs) functionalized with TEMPO radicals.[32] In particular, hydrophilic moieties were introduced onto the large rim of the CD cavity by a thiol-ene reaction while the TEMPO units were attached on the small rim by a copper(I) azide-alkine click reaction (see **CD2** in the scheme of Figure 1). The compound **CD2** was tested for the *in vivo* imaging of glioma-bearing rats and the results were compared with gadolinium diethylenetriaminepentaacetate (Gd(DTPA)) at the same dose (0.2 mmol kg^{-1}). As a positive result, a good uptake of **CD2** into the tumor mass was observed and the compound was well tolerated by the animal without significant side effects. Anyway, Gd(DTPA) showed, as expected, a better contrast enhancement compared to **CD2** whose performance was limited by the short lifetime of the radicals once introduced into the animal body. However, it was interesting to observe that T_1 reduction after the injection of **CD2** lasted for a time longer than 4-hydroxy-TEMPO (at the same concentration of radicals). Indeed, 4-hydroxy-TEMPO was quickly reduced. Thus, it seemed that attaching TEMPO radicals on the CD cavity may have had some beneficial effects on their stability to reduction. Following that approach and intrigued by the first results we have decided to investigate further that class of molecules also considering a change of the kind of nitroxide attached on the CD cavity (compounds **CD3**, **CD4** and **CD5** reported in Figure 1). Considering the strong participation of the NRs to the redox chains in the biological media, in the present work, we have carried out a detailed characterization of the redox properties of the compounds **CD2**–**CD5** by using electron paramagnetic resonance (EPR) spectroscopy and cyclic voltammetry (CV). A comparison with the corresponding mononitroxides is also provided. In view of their biological application, the cytocompatibility of the compounds **CD2**–**CD5** has been tested *in vitro* on three different cell lines, HEK293 human embryonic kidney cells, L929 mouse fibroblasts and U87 glioblastoma cells. Finally, the *in vivo* MRI application of the compounds **CD3**–**CD5** has been investigated and the results are hereafter discussed.

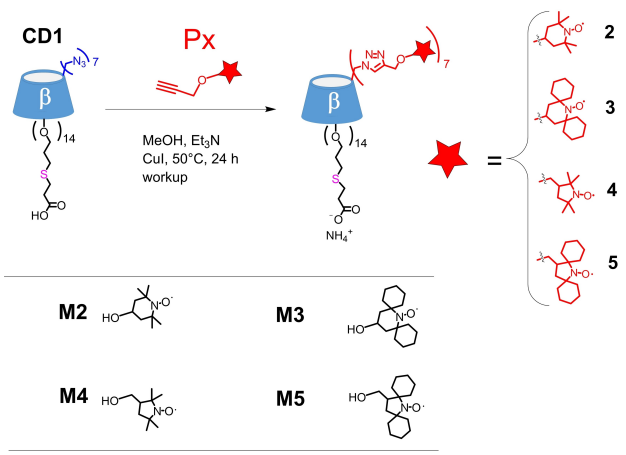

Figure 1. Synthesis of the cyclodextrin-polynitroxide compounds **CD2**–**CD5** and molecular structures of the mononitroxides **M2**–**M5**. Molecular weights: **CD2** and **CD4**: 5067.45 g mol^{-1}; **CD3** and **CD5**: 5623.80 g mol^{-1}.

Results and Discussion

Figure 1 reports a scheme for the synthesis of CD-polynitroxides investigated in this work. The starting material is represented by the compound **CD1** whose synthesis was reported in a previous paper.[32] Different nitroxides with a terminal alkyne group were prepared (compounds **P2**–**P5**, see SI file for details). The final products were obtained smoothly by azide-alkyne click chemistry followed by an easy work-up to obtain water-soluble derivatives. The nitroxides in the compounds **CD2** and **CD3** have a piperidine ring whereas those in **CD4** and **CD5** have a pyrrolidine ring. According to the literature indeed, nitroxides with five-member rings have a significantly longer persistence in presence of a reducing environment as compared to those having a six-member ring. While this aspect has been well investigated in the case of small molecular weight nitroxides,[28,29] supramolecular compounds, like those proposed in this work, have not received a similar consideration as far as we know.

A few years ago, Ionita et. al. investigated nitroxide radicals and biradicals complexed with CDs, and the complexation equilibria were monitored by EPR lineshape analysis.[33,34] In those studies, the weak host-guest interactions and the ensuing small binding constants caused in many cases a substantial presence of unbound nitroxides in solution. Bagryanskaya et al. carried out a detailed EPR study on fully methylated CDs monofunctionalized with different kind of nitroxides having piperidine, pyrroline, pyrrolidine and imidazoline structure. In particular, the CD functionalized with the imidazoline nitroxide was pH-sensitive but the stability against the reduction by ascorbic acid was not improved.[35]

In the present work we have carried out a detailed characterization of the compounds **CD2**–**CD5** by EPR spectroscopy together with the corresponding mononitroxides (**M2**–**M5**). The room temperature EPR spectra of all the compounds in buffered water solution (PBS, pH 7.4) are characterized by the presence of multiple lines due to the hyperfine interaction of the unpaired electrons with the nitrogen nuclei of the nitroxide groups. The

spectra are reported in Figure 2. The EPR spectra of the mononitroxides **M2**–**M4** show three lines characteristic of an interaction with a single nitrogen atom. Those having the cyclohexyl-group (**M3** and **M5**) have a larger linewidth with respect to **M2** and **M4** because of two reasons: a larger number of ring protons weakly interacting with the unpaired electron, and a larger hydrodynamical dimension. This last property affects the rotational mobility of the molecules, and the slowing down of the tumbling motion generally induces a decrease of transverse spin relaxation time T_2 and consequently an increase in the EPR linewidth. The hyperfine coupling constants are 16.9 Gauss for the tetramethyl-substituted nitroxides and 16.1 Gauss for the cyclohexyl-substituted nitroxides. All these values are in agreement with the hyperfine constants reported for similar compounds in water.[28,36]

The cyclodextrin-polynitroxide compounds **CD2**–**CD5** show EPR spectra with broader lines. As discussed for the monomers, also for these compounds, a bulkier dimension is associated to a broadening of the EPR lines. Additionally, electron-electron spin exchange interactions between the unpaired electrons of nearby nitroxide groups also cause line broadening. Both these mechanisms increase the electron spin relaxation, and they are beneficial for their application as nuclear spin relaxation agents, as confirmed by the relaxivity measurements reported below on **CD2**–**CD5**.

In some spectra of cyclodextrin-polynitroxides, both narrow and large components seem to be present, due to the presence of time-dependent magnetic interactions between two or more nitroxide groups.[37] The presence of non-negligible intramolecular spin-interactions and their role in affecting the magnetic properties of a simplified class of CD-based polynitroxides were already pointed out in previous papers.[32,38] The nitroxide chemical stability in the physiological antioxidant environment can be assessed by measuring the nitroxide disappearance rate when it is converted into the corresponding hydroxylamine by reaction with ascorbic acids. The final products of the reaction are diamagnetic and therefore EPR silent. The method for the determination of the kinetic constant for the second order reaction is described in the Experimental section. An example of experimental results is shown in Figure SI3, and all the calculated kinetic constants are reported in Table 1. From the data reported in Table 1, it is possible to observe trends. As expected, the five-member rings mononitroxides (**M4** and **M5**) show a higher stability (smaller kinetic constant) with respect to reduction by ascorbate, and the cyclohexyl-substituted nitroxides are more stable than the tetramethyl-substituted ones, due to the increased steric protection of the N–O fragment by the bulkier cyclohexyl groups.

More interesting is the comparison between the single nitroxides and the corresponding cyclodextrin-polynitroxide compounds. In all cases, the compounds with a pyrrolidine ring are significantly more resistant to ascorbate reduction among the series of compounds.

A possible reason of the increased stability of all **CD2**–**CD5** compounds might be due to a sort of steric hindrance of the nitroxide units when they are crowded on the rim of the cyclodextrins. This aspect might prevent the diffusion of ascorbate to the nitroxide groups. With respect to this point we can also prefigure a higher organization of the chains bearing the nitroxides for **CD5**, which seems to have larger exchange interactions with respect to other CD derivatives. Secondly, the decrease of diffusional constant of the bulky **CD2**–**CD5** molecules in solution could also affect the rate of reaction. Finally, they are more thermodynamically stable than the corresponding mononitroxide molecules (see further).

A qualitative conclusion from the kinetic analysis of the ascorbate/CD reaction is that the half-lives of the **CD2**–**CD5** in 1 mM water solution of ascorbic acid at pH = 7.4 are longer than those of the single nitroxide precursors (slightly for five-membered rings and significantly for six-membered rings). The retention of short T_1 relaxation time due to improved CA stability during ascorbate reduction was also confirmed using MRI at 9.4 T (Figure SI32).

In order to get more information on the redox properties of the **CD2**–**CD5** and of the corresponding mononitroxides both the oxidation and the reduction of the radicals were studied by cyclic voltammetry (CV) in water. Representative CV profiles for both mononitroxides and cyclodextrin-polynitroxides are provided in Figure SI5, whereas the redox parameters extracted from the CVs are collected in Table SI2.

The CVs show a reversible peak couple near 0.5 V related to the reversible oxidation of $RNO^{\bullet}$ to RNO^{+}. All compounds

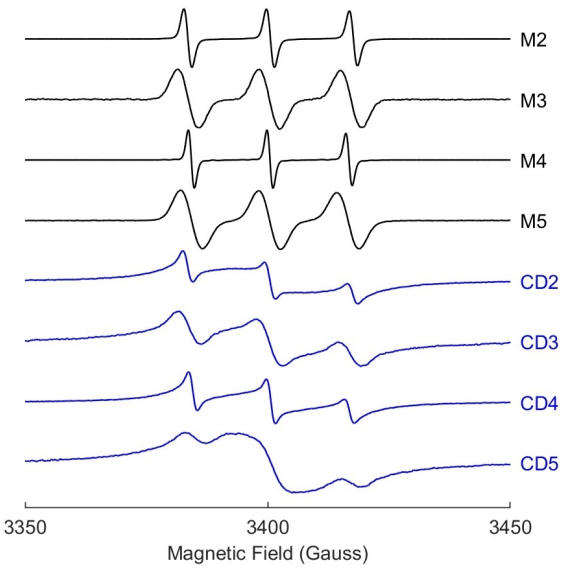

Figure 2. EPR spectra of mononitroxides **M2**–**M5** (black lines) and of the corresponding cyclodextrin-nitroxides **CD2**–**CD5** (blue lines) in water/PBS at room temperature.

Table 1. Second order kinetic constants of the Ascorbic acid/Nitroxide reaction in H_2O/PBS measured at room temperature. The relative error on each value is estimated to be ±30%. (black: mononitroxides, blue: cyclodextrin-nitroxides).

Second order kinetic constant ($M^{-1}s^{-1}$)	**M2**	**M3**	**M4**	**M5**
	7.9	1.4	0.04	0.08
	CD2	**CD3**	**CD4**	**CD5**
	3.5	0.5	0.04	0.05

exhibited this reversible oxidation wave except **CD3** for which the oxidation process was irreversible.

Unlike the oxidation process, observed for all compounds, a reduction peak in water could be observed only for mononitroxides **M2**–**M5**. Additionally, no anodic peak for the reoxidation of electrogenerated RNO^- could be observed, clearly indicating that this last species is unstable and possibly decays via fast protonation and/or ring opening. Analysis of the effect of the scan rate demonstrated that reduced mononitroxides not only decay rapidly but also their generation involves a slow electron transfer.

For all cyclodextrin-polynitroxides, instead, the reduction wave was masked by the reduction of water (the hydrogen evolution reaction). Indeed, all cyclodextrin-polynitroxide radicals have a negative charge and, as expected, their reduction potentials are more negative than those of the corresponding mono-radicals.

The reduction potentials of cyclodextrin-nitroxide radicals could not be measured in H_2O, where, on the contrary, the oxidation potentials were determined for the whole series. However, the reduction potentials are more relevant than the oxidation potentials for the comparison with the kinetics of reduction by ascorbic acid. Therefore, we also examined the cyclic voltammetry of all radicals in DMF, a solvent with a cathodic discharge potential lower than that of water and with good solubility properties for all investigated nitroxide radicals.

Figure SI5 reports the CVs recorded at $v = 0.1$ V/s for the reduction of all compounds in DMF. In this solvent, a single irreversible reduction peak is observed for all compounds (the peak potentials are reported in Table SI3). The presence of a single cathodic peak for the cyclodextrin-polynitroxides suggests that all nitroxyl units in the molecules are electrochemically equivalent and therefore undergo reduction at the same potential; in other words, all nitroxide moieties attached to a CD framework behave in the same way and do not present discernible differences in redox properties. As in water, voltammetric analysis of the cathodic peak has shown that the reduction process involves a slow electron transfer, followed by chemical decay of the electrogenerated species. CVs of all mononitroxide radicals showed small anodic peak(s) attributed to the oxidation of products arising from decomposition of electrogenerated RNO^-.

The reduction potentials, E_{pc}, of the nitroxides depend on three factors, namely (i) whether RNO is free or linked to a cyclodextrin, (ii) the alkyl ring of the RNO radical and (iii) the protection group (methyl vs cyclohexyl). Some general trends, one for each factor, can be observed provided that the effect of each factor is examined while keeping constant the other two factors. Methyl substituted radicals have higher (less negative) reduction potentials than radicals bearing cyclohexyl groups (0.02–0.12 V); an exception from this trend was observed for the **CD4** and **CD5** couple. Reducing the ring size from a six-membered ring to a five-membered one shifts E_{pc} to higher values (0.03–0.33 V). Last, cyclodextrin-polynitroxides show E_{pc} values that are lower by 0.09–0.31 V than those of the corresponding mononitroxides. This last trend is not surprising because cyclodextrins bear a large negative charge for the presence of the charged side chains, which opposes to the incoming negative charge upon reduction.

Next, we examined the correlation between the kinetic constants for the reduction of nitroxide radicals by ascorbic acid and their reduction potentials.

Since the reduction potentials of cyclodextrin-polynitroxides could not be measured in water, the E_{pc} values obtained in DMF were used, assuming that a change of solvent does not affect the trend of reduction potentials. A plot of the log(k) as a function of E_{pc}, which is related to the standard reduction potential, is displayed in Figure 3. A fairly linear correlation between log(k) and E_{pc} is observed if the compounds are separated into two groups, one for the cyclodextrin-polynitroxides and another for the mononitroxides.

Within each group, the lower the reduction potential, the lower the kinetic constant, i.e., a greater nitroxide radical stability. It can be observed that the cyclodextrin-polynitroxides are on average in the left part of the plot (lower reduction potential), and the mononitroxides are in the right part (higher reduction potential). **CD5** seems to be out of the trend, indicating that multiple factors contribute to the chemical inertia of the system. One of these might be a different organization of the chains of the CD core bearing the nitroxides that might be responsible for an extra line broadening of the EPR linewidth (see Figure 2), suggesting a more compact bundle of chains.

In view of their *in vivo* application, the cytocompatibility of **CD2**–**CD5** was tested *in vitro* using three cell lines, HEK293 human embryonic kidney cells, L929 mouse fibroblasts and U87 glioblastoma cells. The range of concentrations was between 0.125 μmol mL^{-1} and 1 μmol mL^{-1}. The viability of all cell lines incubated with the different concentrations of **CD2**–**CD5** was comparable or higher than those of cells cultured under standard conditions. All values are generally above 70%, limit to consider samples non-cytotoxic according to the EN ISO 10993-12 standard. (Figure 4).[39]

The relaxivity properties (r_1) of the developed compounds were investigated at a clinically and preclinically relevant magnetic field strength (B_0) range because it can vary depend-

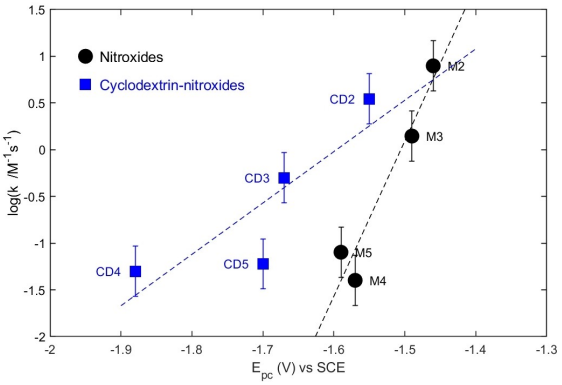

Figure 3. Correlation plot between the reduction potentials of nitroxide radicals in DMF and the logarithm of the rate constants for their reaction with ascorbate. The dotted lines are introduced only for a better visualization of the data.

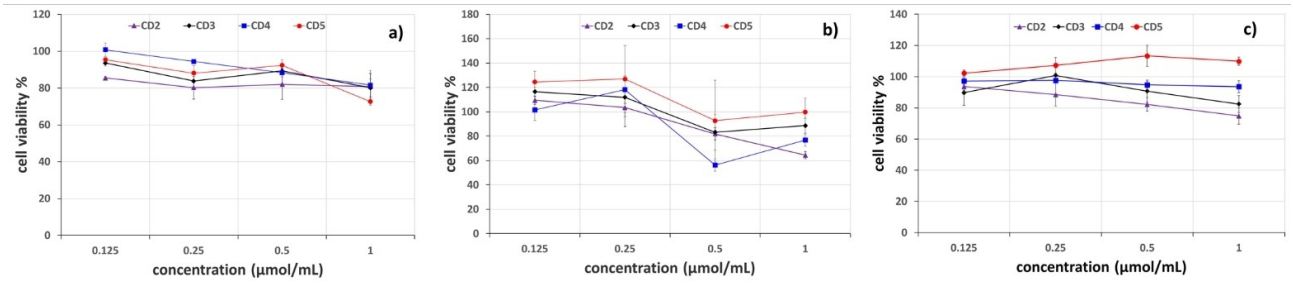

Figure 4. Cell viability: a) HEK293 kidney cells; b) L929 fibroblasts; c) U87 glioblastoma cells. The lines connecting the points are only for a better visualization of the experimental data

ing on the CA structure. The r_1 varied from 0.6 to 0.9 $s^{-1}mM^{-1}$ for different compounds at 9.4 T and generally increased as magnetic field B_0 decreased (see Table 2). This is consistent with the overall dependence of r_1 on B_0 known from literature,[40] but here the interesting result is that the compound **CD4** having a pyrrolidine ring and four methyl groups appears to be less sensitive to B_0 variation than **CD3** and **CD5** having a piperidine ring and four methyl groups. This could have implications for further development as the clinical practice is translating from 1.5 T to 3 T. The CAs were then tested in a glioma model in rats. Average T_1 relaxation times (n = 5) before injection were 2.25 ± 0.08 s, 1.74 ± 0.05 s and 1.91 ± 0.11 s in tumor, brain and the surrounding muscle, respectively.

Following **CD** injection, average tumor T_1 decreased until around 20 mins post-injection (Figure 5) reaching 1.87 ± 0.07 s (n = 4, ΔT_1 −0.37 ± 0.13 s) and remaining low until the end of the 60 min follow-up period. In comparison, in our previous study using **CD2**, the overall T_1 change was smaller and tumor T_1 had returned to baseline at the same time.[32] GdDTPA injection caused a T_1 decrease to 0.78 ± 0.06 s (n = 3) at ~8 min post-injection with recovery, with one animal showing minimal subsequent recovery suggesting some pooling of contrast agent to the tumor. There was a small T_1 decrease in the normal brain tissue during the first 10 mins post-**CDx** injection after which the value returned to pre-injection value. In muscles **CDx** injection also led to a decrease in T_1 followed by a slow recovery.

Correcting for the differing relaxivities, these T_1 values correspond to apparent peak concentrations of 0.08 ± 0.01 mM (0.16 ± 0.00 %ID/g), 0.20 ± 0.03 mM (0.37 ± 0.05 %ID/g) and 0.19 ± 0.02 mM (0.38 ± 0.03 %ID/g) for **CD4**, **CD3** and GdDTPA, respectively. While the variable leakiness of tumors is likely to contribute to the observed difference, the results suggest a preferential tumor contrast retention with **CD3** despite its somewhat faster reduction rate.

Animal receiving **CD5** died unexpectedly 15 min post-injection raising a question about toxicity. A non-tumor bearing rat receiving **CD5** showed normal physiological behavior. Therefore, while we cannot rule out a potential toxic effect of **CD5**, death was more likely due complications from the aggressive tumor burden rather than CA itself. Nevertheless, further safety studies will be warranted in the next generation of contrast agents to identify any potential adverse effects. In the non-tumor-bearing rat, the volume coil was placed around kidney and bladder to investigate the removal of contrast agent. T_1 of kidneys was reduced from 1.7 s to 0.9 s upon injection of **CD5** and slowly recovered but remained low throughout the observation period reaching 1.2 s by the end of it (Figure SI33). The amount of CA was increasing in the bladder suggesting at least a partial removal of contrast agent through the kidneys. Taken together, the results show that the new CAs show improved *in vivo* performance, most likely owing to higher stability against reducing agents.

Table 2. T_1 (s) and relaxivities ($s^{-1}mM^{-1}$) of 5 mM and 0.5 mM contrast agent solutions at 20 °C.

5 mM	T_1 (s)				r ($s^{-1}mM^{-1}$)		
B_0 (T)	Saline	**CD3**	**CD4**	**CD5**	**CD3**	**CD4**	**CD5**
0.7	2.22	0.10	0.13	0.10	1.89	1.48	1.93
3	2.61	0.17	0.18	0.15	1.08	1.02	1.24
7	2.69	0.25	0.19	0.19	0.71	0.97	0.96
9.4	2.67	0.30	0.22	0.22	0.59	0.84	0.83
0.5 mM	T_1 (s)				r ($s^{-1}mM^{-1}$)		
B_0 (T)	Saline	**CD3**	**CD4**	**CD5**	**CD3**	**CD4**	**CD5**
0.7	2.28	0.73	0.87	0.68	1.85	1.39	2.03
3	2.40	1.07	1.09	0.96	1.02	0.99	1.22
7	2.48	1.35	1.20	1.22	0.67	0.87	0.82
9.4	2.54	1.44	1.19	1.31	0.60	0.88	0.73

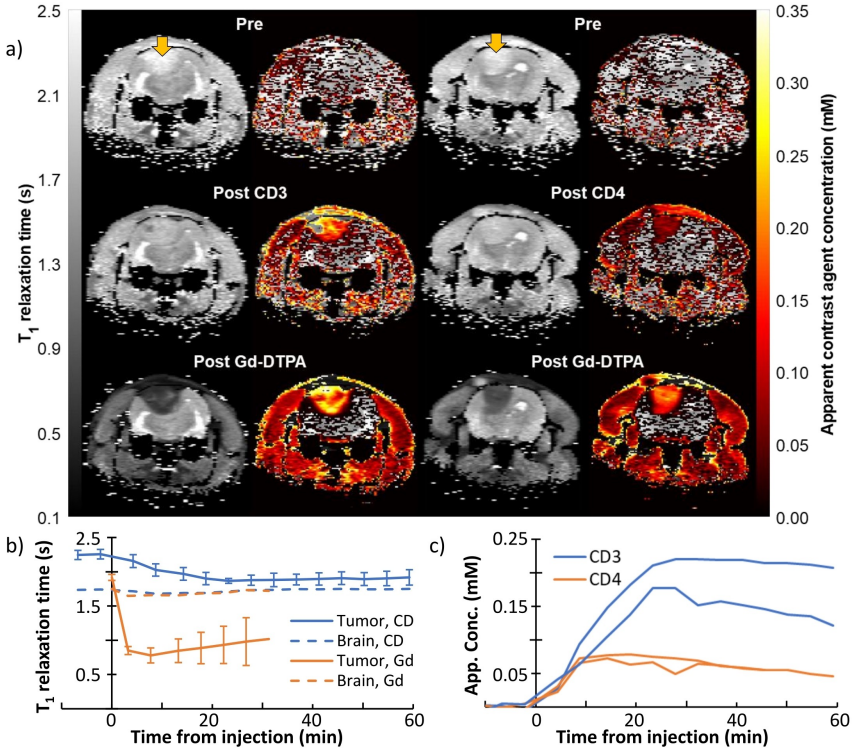

Figure 5. In vivo MRI. T_1 relaxation time maps measured in rats bearing C6 brain tumor (tumor indicated with yellow arrow in pre-contrast images) before and after CA injection (A), T_1 time courses (B) and corresponding apparent CA concentrations calculated from measured relaxation time changes and relaxivities (C). Data for two animals is shown, each animal received injections of either **CD3** or **CD4** followed by Gd-DTPA 60 mins later. In (C) all individual animals are shown with color indicating the used CA. Injection of CD or Gd-DTPA leads to a T_1 reduction within tumor as the contrast agent pools inside the tumor due to leaky blood vessels. The contrast was retained for at least 60 mins.

Conclusions

CAs for MRI based on organic radicals (typically TEMPO) are a potential alternative to those based on Gd(III) complexes but their use in the clinical practice is still limited by their low stability *in vivo*. In order to overcome such limitations, a set of water-soluble supramolecular polynitroxides has been designed and developed from β-CD through a suitable combination of thiol-ene and copper(I)-catalyzed alkyne-azide "click reactions". The radical moieties have been introduced on the small rim of β-CD molecule while the large rim has been functionalized with polar arms ending with carboxylic groups. Both nitroxides with a piperidine structure (**CD2** and **CD3**) and with a pyrrolidine structure (**CD4** and **CD5**) have been considered in order to get derivatives having a different stability in presence of a reducing environment. The redox properties of the proposed compounds have been investigated by EPR spectroscopy and cyclic voltammetry and a comparison with the corresponding mononitroxides is provided. With regard to the reduction test in presence of ascorbic acid, the compounds **CD4** and **CD5** have very low second order kinetic constants making them very promising for *in vivo* applications. Moreover, we have found a general lowering of this parameter compared to the corresponding mononitroxides (**M2**–**M5**). The lowering is particularly evident with compounds **CD2** and **CD3** for which the kinetic constant is half the value found for **M2** and **M3** respectively. Therefore, a beneficial effect is obtained by covalently fixing nitroxides on a supramolecular scaffold. Tests *in vitro* on HEK293 human embryonic kidney cells, L929 mouse fibroblasts and U87 glioblastoma cells showed that all compounds can be considered non-cytotoxic in a range of concentration comprised between 0.125 $\mu mol\,mL^{-1}$ and 1 $\mu mol\,mL^{-1}$. The compounds **CD3**–**CD5** have been tested by *in vivo* MRI at 9.4 T in a glioma model in rats and compared with Gd-DTPA as standard. The experiments showed a good lowering in tumor T_1 relaxation and an improved retention of the contrast for at least 60 mins. CAs are removed at least partially via kidneys.

Experimental Section

The compounds **CD1** and **CD2** were synthesized following a procedure reported in the literature.[32] The compounds **CD3**, **CD4** and **CD5** were obtained in a way similar to **CD2**. The details of their synthesis and characterization are reported in the Supporting Information, together with the procedures for the synthesis of the remaining nitroxides, including the intermediates.

EPR Spectroscopy

EPR measurements were carried out at room temperature in a Bruker ECS spectrometer, using 1 mm diameter capillary tubes and the following parameters: microwave power 2 mW, modulation amplitude 1 Gauss, sweep width 150 Gauss. For the EPR spectra of the cyclodextrin-polynitroxides **CD2**–**CD5** and the mononitroxides **M2**–**M5**, the radicals were dissolved in water/PBS buffer (pH = 7.4)

at a concentration of 10^{-4} M. Ascorbic acid solutions in PBS were prepared at a concentration 10^{-2} M, i.e., up to 100 times higher than the concentration of the nitroxides. Equal volumes of nitroxide and ascorbate solutions were mixed to a final nitroxide concentration of 5×10^{-5} M and the EPR spectra were recorded as a function of time. From the single exponential fitting of the decaying EPR intensity, the pseudo first-order rate constant is obtained, and the second-order kinetic constant is calculated by dividing the pseudo first-order rate constant by the ascorbate concentration. To obtain a more robust estimate of the second-order constant, the pseudo first-order kinetic analysis was repeated at different initial ascorbate concentrations, always in large excess compared to the nitroxide initial concentration.

CV Experiments

For cyclic voltammetry measurements in doubly distilled water, solutions of all samples were prepared at a radical concentration in the range 1–2 mM. The pH was fixed at a value of 7.5 ± 0.5 by means of a carbonate buffer at a concentration of 0.1 M. Potentials were measured with respect to saturated calomel electrode (SCE) in an electrochemical cell deoxygenated by an Ar flow. The counter electrode was a Pt wire, while the working electrode was a polished glassy carbon disc.

For CV measurements in DMF the same working and counter electrodes were used, together with a reference electrode made of Ag/AgI in 0.1 M Bu_4NI in DMF. This reference electrode was constantly calibrated versus the ferrocenium/ferrocene (Fc^+/Fc) redox couple used as an internal standard. Then the potentials measured versus Ag/AgI, were converted to the saturated calomel scale by using $E^\circ_{Fc^+/Fc}=0.476$ V vs SCE.

Cytocompatibility Tests

Samples were dissolved in complete culture medium at 4 different concentrations (0.125 μmol/mL to 1 μmol/mL). Indirect cytotoxicity tests were performed in accordance with the ISO 10993-12:2009 standard.[39] Dulbecco's Modified Eagle Medium (DMEM) supplemented with 1 mM sodium pyruvate, 10 mM HEPES buffer, 100 U mL^{-1} penicillin, 0.1 mg mL^{-1} streptomycin, 2 mM glutamine, and 10% (v/v) fetal bovine serum (FBS) was used to dissolve the compounds at different concentrations. Three different cell lines were used: L929 murine fibroblast, HEK293 human embryo kidney and U87 glioblastoma cells. All cell lines were seeded in a 96-well culture plate (10^4 cells/well, in 100 μL of complete DMEM) and incubated in standard culture conditions for 24 h. Afterwards, the medium was replaced with 100 μL/well of each prepared solution (n = 3 wells/concentration/cell), and the plate incubated for further 24 h in standard culture conditions. Cells cultured in complete DMEM were used as control (CTRL, n = 3). Cell viability was assessed using resazurin assay (Sigma Aldrich). Fluorescence ($\lambda_{ex}=540$ nm; $\lambda_{em}=595$ nm) was measured with a Synergy H1 spectrophotometer (BioTek, Italy). For each well, cell viability was calculated using the following equation (1):

$$Viability\ (\%) = \left[\frac{RFU_{sample} - RFU_{resazurin}}{RFU_{CTRL} - RFU_{resazurin}}\right] \times 100 \quad (1)$$

where RFU_{sample}, $RFU_{resazurin}$, and RFU_{CTRL} are the fluorescence of the sample, of resazurin, and control, respectively.

Magnetic Field Dependence of CA Relaxivity

Saline samples containing 5 mM or 0.5 mM of each contrast agent (**CD3**, **CD4** and **CD5**) were prepared and measured along with saline control at main magnetic fields 0.7 T, 3 T, 7 T and 9.4 T and at 20 degrees. Experiments at 9.4 T were performed using Agilent (Palo Alto, US) imaging system whereas the other measurements were performed using a MR Solutions (Guildford, UK) imaging system with an adjustable field strength. In both systems, a transmit/receive volume coil was used for data collection with Look-Locker-type gradient echo imaging pulse sequence (flip angle 8 degrees, matrix 64×32). Two datasets were collected to account for the T_1 difference between saline and samples containing contrast agents. Inversion times were spaced 200 ms apart for saline experiment, and 10 ms (0.7 T, 3 T or 7 T) or 50 ms (9.4 T) for CA experiment. Data were fitted to monoexponential equations incorporating the apparent change in T_1 due to Look-Locker approach.

In Vivo MRI

All animal experiments were approved by the Animal Health Welfare and Ethics Committee of University of Eastern Finland. The methods used were similar to those described in literature.[30,41] Briefly, female Wistar rats (N = 6, 230–270 g, Envigo) were implanted with 10^6 C6 glioma cells (ECACC/Sigma Aldrich) to stereotactic coordinates of 1 mm caudal from bregma, 2 mm to the right of sagittal suture and 2 mm below the top of bregma through a burr hole. Tumors were allowed to grow for 10 days before the experiment at which point five animals had developed a tumor. Isoflurane-anesthetized animals (5% induction, 1–2% upkeep, 70:30 N_2:O_2 gas mixture at 2 L/min) with physiological monitoring (60-80 breaths per minute, 37 degrees Celsius) were imaged at 9.4 T (Agilent, Santa Clara, US) using a volume coil transmitter/quad surface coil receiver pair (Rapid Biomedical, Rimpar, Germany). Data from tumor and normal brain tissue were collected before and for up to one hour after the tail vein injection of the contrast agent using an axial (field of view 32x32 mm^2 covered with 128x64 data matrix) multi-slice T_1 relaxation map pulse sequence (inversion-recovery FLASH with repetition time of 7.8 ms and echo time of 3.9 ms, flip angle 10 degrees, twelve 1 mm slices, 12 inversion times between 5 and 5500 ms, 10 s recovery delay).

Two tumor-bearing animals were imaged using **CD4** and **CD3** and one tumor-bearing animal was imaged using **CD5**, all at 0.2 mmol/kg final concentration (injection rate 2.2 ml/min). Three of the animals received a subsequent injection of Gd(DTPA), 0.2 mmol/kg, 60 minutes after the first injection. All relaxation maps were calculated as monoexponential fits in Matlab (Mathworks, Natick, US) and regions of interest from tumor and normal brains were analysed. In one animal with no tumor, **CD5** at 0.2 mmol/kg was injected, and T_1 changes in kidney and bladder were observed for 2.5 hours to assess CA clearance.

Supporting Information

The authors have cited additional references within the Supporting Information.[42]

Author Contributions

LF, AAI, AB: EPR and cyclic voltammetry experiments; LA: *in-vitro* testing; VH, JR, VO, MK: animal handling, *in-vivo* MRI experi-

ments; LM: conceptualization, design and synthesis of the compounds, overall coordination. All authors contributed to writing the manuscript and approved it for publication.

Acknowledgements

Financial support from Academy of Finland (grant no. 332006) is gratefully acknowledged. The authors acknowledge Euro-BioImaging (www.eurobioimaging.eu) for providing access to imaging technologies and services via the Finnish Biomedical Imaging Node (Kuopio Biomedical Imaging Unit, part of Biocenter Kuopio, University of Eastern Finland, Kuopio, Finland).

Conflict of Interests

The authors declare no conflict of interest.

Data Availability Statement

The data that support the findings of this study are available in the supplementary material of this article.

Keywords: cyclodextrin · contrast agents · glioma · MRI imaging · nitroxides

[1] L. Helm, A. E. Merbach, É. Tóth, *The Chemistry of Contrast Agents in Medical Magnetic Resonance Imaging*, Second edition, Wiley **2013**, ISBN: 978–1-119-99176-2.
[2] S. C. Bushong, G. Clarke, *Magnetic Resonance Imaging: Physical and Biological Principles*, Fourth edition, Elsevier **2015**, ISBN: 978–0-323-07354-7.
[3] Caravan, J. J. Ellison, T. J. McMurry, R. B. Lauffer, *Chem. Rev.* **1999**, *99*, 2293–2352.
[4] A. J. L. Villaraza, A. Bumb, M. W. Brechbiel, *Chem. Rev.* **2010**, *110*, 2921–2959.
[5] T. J. Fraum, D. R. Ludwig, M. R. Bashir, K. J. Fowler, *J. Magn. Reson. Imaging* **2017**, *46*, 338–353.
[6] T. Kanda, Fukusato, M. Matsuda, K. Toyoda, H. Oba, J. Kotoku, T. Haruyama, K. Kitajima, S. Furui, *Radiology* **2015**, *276*, 228–232.
[7] R. Pullicino, M. Radon, S. Biswas, M. Bhojak, K. Das, *Clin. Neuroradiol.* **2018**, *28*, 159–169.
[8] "EMA's final opinion confirms restrictions on use of linear gadolinium agents in body scans", EMA2017, can be found under http://www.ema.europa.eu/en/medicines/human/referrals/gadolinium-containing-contrast-agents.
[9] B. P. Soule, F. Hyodo, K.-i. Matsumoto, N. L. Simone, J. A. Cook, M. C. Krishna, J. B. Mitchell, *Free Radical Biol. Med.* **2007**, *42*, 1632–1650.
[10] A. Rajca, Y. Wang, M. Boska, J. T. Paletta, A. Olankitwanit, M. A. Swanson, D. G. Mitchell, S. S. Eaton, G. R. Eaton, S. Rajca, *J. Am. Chem. Soc.* **2012**, *134*, 15724–15727.
[11] O. U. Akakuru, M. Z. Iqbal, M. Saeed, C. Liu, T. Paunesku, G. Woloschak, N. S. Hosmane, A. Wu, *Bioconjugate Chem.* **2019**, *30*, 2264–2286.
[12] C. Fu, Y. Y. Xin Xu, Q. Wang, Y. Chang, C. Zhang, J. Zhao, H. Peng, A. K. Whittaker, *Prog. Polym. Sci.* **2020**, *108*, 101286.
[13] M. Tweedle, *Invest. Radiol.* **2021**, *56*, 35–41.
[14] E. Mauri, E. Micotti, A. Rossetti, L. Melone, S. Papa, G. Azzolini, S. Rimondo, P. Veglianese, C. Punta, F. Rossi, A. Sacchetti, *Soft Matter* **2018**, *14*, 558–565.
[15] Y. Zhu, Y. Matsumura, M. Velayutham, L. M. Foley, T. K. Hitchens, W. R. Wagner, *Biomaterials* **2018**, *177*, 98–112.
[16] K.-I. Matsumoto, I. Nakanishi, Z. Zhelev, R. Bakalova, I. Aoki, *Antioxid. Redox Signaling* **2022**, *36*(1–3), 95–121 and references therein.
[17] V.-T. Nguyen, A. Detappe, N. M. Gallagher, H. Zhang, P. Harvey, C. Yan, C. Mathieu, M. R. Golder, Y. Jiang, M. F. Ottaviani, A. Jasanoff, A. Rajca, I. Ghobrial, P. P. Ghoroghchian, J. A. Johnson, *ACS Nano* **2018**, *12*, 11343–11354.
[18] O. U. Akakuru, M. Z. Iqbal, C. L. J. Xing, Z. Wei, Z. Jiang, Q. Fang, B. Yuan, E. I. Nosike, J. Xia, Y. Jin, J. Zheng, A. Wu, *Appl. Mater. Today* **2020**, *18*,100524.
[19] S. Guo, X. Wang, Y. Dai, X. Dai, Z. Li, Q. Luo, X. Zheng, Z. Gu, H. Zhang, Q. Gong, K. Luo, *Adv. Sci.* **2020**, *7*,2000467.
[20] H. Lee, A. Shahrivarkevishahi, J. L. Lumata, M. A. Luzuriaga, L. M. Hagge, C. E. Benjamin, O. R. Brohlin, C. R. Parish, H. R. Firouzi, S. O. Nielsen, L. L. Lumata, J. J. Gassensmith, *Chem. Sci.* **2020**, *11*, 2045–2050.
[21] H. V.-T. Nguyen, A. Detappe, P. Harvey, N. Gallagher, C. Mathieu, M. P. Agius, O. Zavidij, W. Wang, Y. Jiang, A. Rajca, A. Jasanoff, I. M. Ghobrial, P. P. Ghoroghchian, J. A. Johnson, *Polym. Chem.* **2020**, *11*, 4768–4779.
[22] L. F. Pinto, V. Lloveras, S. Zhang, F. Liko, J. Veciana, J. L. Muñoz-Gómez, J. Vidal-Gancedo, *ACS Appl. Bio Mater.* **2020**, *3*, 369–376.
[23] S. Zhang, V. Lloveras, D. Pulido, F. Liko, L. F. Pinto, F. Albericio, M. Royo, J. Vidal-Gancedo, *Pharmaceutica* **2020**, *12*, 772.
[24] O. U. Akakuru, C. Xu, C. Liu, Z. Li, J. Xing, C. Pan, Y. Li, E. I. Nosike, Z. Zhang, Z. M. Iqbal, J. Zheng, A. Wu, *ACS Nano* **2021**, *15*, 3079–3097.
[25] S. Guo, X. Wang, Z. Li, D. Pan, Y. Dai, Y. Ye, X. Tian, Z. Gu, Q. Gong, H. Zhang, K. Luo, *J. Nanobiotechnol.* **2021**, *19*, 244.
[26] X. Wang, S. Guo, Z. Li, Q. Luo, Y. Dai, H. Zhang, Y. Ye, Q. Gong, K. Lu, *J. Nanobiotechnol.* **2021**, *19*, 205.
[27] Z. Peng, X.-Q. Xu, X.-Q. Wang, X. Shi, W. Wang, H.-B. Yang, *Chem. Commun.* **2022**, *58*, 2006–2009.
[28] I. A. Kirilyuk, Y. F. Polienko, O. A. Krumkacheva, R. K. Strizhakov, Y. V. Gatilov, I. A. Grigor'ev, E. G. Bagryanskaya, *J. Org. Chem.* **2012**, *77*, 8016–802.
[29] J. T. Paletta, M. Pink, B. Foley, S. Rajca, A. Rajca, *Org. Lett.* **2012**, *14*, 5322–5325.
[30] M. Soikkeli, M. I. Kettunen, R. Nivajärvi, V. Olsson, S. Rönkkö, J. P. Laakkonen, V.-P. Lehto, J. Kavakka, S. Heikkinen, *Contrast Media Mol. Imaging* **2019**, Article ID 5629597.
[31] J. Ju, D. Xu, X. Mo, J. Miao, L. Xu, G. Ge, X. Zhu, H. Deng, *Carbohydr. Polym.* **2023**, *317*, 121048.
[32] L. Melone, A. Bach, G. Lamura, F. Canepa, R. Nivajärvi, V. Olsson, M. Kettunen, *ChemPlusChem* **2020**, *85*, 1171–1178.
[33] G. Ionita, V. Meltzer, E. Pincu, V. Chechik, *Org. Biomol. Chem.* **2007**, *5*, 1910–1914.
[34] G. Ionita, A. Caragheorgheopol, H. Caldararu, L. Jones, V. Chechik, *Org. Biomol. Chem.* **2009**, *7*, 598–602.
[35] O. A. Krumkacheva, M. V. Fedin, D. N. Polovyanenko, L. Jicsinszky, S. R. A. Marque, E. G. Bagryanskaya, *J. Phys. Chem. B* **2013**, *117*, 8223–8231.
[36] G. I. Likhtenshtein, J. Yamauchi, S. Nakatsuji, A. I. Smirnov, R. Tamura, *Nitroxides: Applications in Chemistry, Biomedicine, and Materials Science*, Wiley, **2008**.
[37] S. S. Eaton, L. B. Woodcock, G. R. Eaton, *Concepts Magn. Reson. Part A* **2019**, *47A*, e21426.
[38] F. Caglieris, L. Melone, F. Canepa, G. Lamura, F. Castiglione, M. Ferro, L. Malpezzi, A. Mele, C. Punta, P. Franchi, M. Lucarini, B. Rossi, F. Trotta, *RSC Adv.* **2015**, *5*, 76133–76140.
[39] ISO 10993–12:2021 "Biological evaluation of medical devices – Part 12: Sample preparation and reference materials" can be found under http://www.iso.org/standard/75769.html.
[40] P. Caravan, C. T. Farrar, L. Frullano, R. Uppal, *Contrast Media Mol. Imaging* **2009**, *4*, 89–100.
[41] R. Nivajärvi, V. Olsson, V. Hyppönen, S. Bowen, H. M. Leinonen, H. P. Lesch, J. H. Ardenkjær-Larsen, O. H. J. Gröhn, S. Ylä-Herttuala, M. I. Kettunen, *NMR Biomed.* **2020**, *33*, e4250.
[42] M. M. Haugland, A. H. El-Sagheer, R. J. Porter, J. Peña, T. Brown, E. A. Anderson, J. E. Lovett, *J. Am. Chem. Soc.* **2016**, *138*, 9069–9072.

Manuscript received: February 8, 2023
Revised manuscript received: July 7, 2023
Accepted manuscript online: July 11, 2023
Version of record online: August 8, 2023